Supporting Information

Construction of orderly hierarchical FeOOH/NiFe layered double hydroxides supported on cobaltous carbonate hydroxide nanowire arrays for highly efficient oxygen evolution reaction

Jun Chi [a,b], *Hongmei Yu* [a,*], *Guang Jiang* [a,b], *Jia Jia* [a,b], *Bowen Qin* [a,b], *Baolian Yi* [a], *and Zhigang Shao* [a,*]

[a] Fuel Cell System and Engineering Laboratory, Dalian Institute of Chemical Physics, Chinese Academy of Sciences, Dalian, 116023, PR China

[b] University of Chinese Academy of Sciences, Beijing, 100049, PR China

E-mail: hmyu@dicp.ac.cn, zhgshao@dicp.ac.cn

**E-mail: hmyu@dicp.ac.cn. zhgshao@dicp.ac.cn*

Tel.: +86-411-84379051;

Fax: +86-411-84379185

S1. Experimental Section.

Chemicals and Materials: Ni foams (4 cm ×8 cm× 1.4 mm) were used as the substrates. Cobalt nitrate hexahydrate (Aladdin, ≥99.5%), urea (Aladdin, ≥99.5%), potassium hydroxide (Aladdin, ≥99.99%) were purchased from Aladdin Chemical Reagent Co. Ltd. Iron nitrate nonahydrate (Damao, ≥98%), Nickel nitrate hexahydrate (Damao, ≥98%), ammonium fluoride (Damao, ≥96%) were purchased from Damao Chemicals and used as received. All the standard solutions were prepared with deionized water with the resistance of 18 MΩ at 25 °C.

Hydrothermal fabrication of CCH NAs-NF: NF was sonicated in HCl solution (10 wt.%) for 10 min to remove the nickel oxides on the surface, and rinsed with deionized water and ethanol for three times. The precursor solution was prepared by dissolving $Co(NO_3)_2$ (4mmol), $CO(NH_2)_2$ (15 mmol) in deionized water (70 mL) followed by 30 min stirring to ensure the homogeneity. The pH of the precursor solution should be carefully controlled around 10. The resultant solution was then transferred into a 80 mL Teflon-lined stainless steel autoclave. NF was immersed into the precursor solution vertically. The autoclave was then sealed and transferred in an electric oven maintained at 120 °C for 5 h. After that, the autoclave cooled down naturally. The resultant sample was rinsed with deionized water and absolute ethanol to remove the residual reactants and dried in air. and accordingly the CCH NAs-NF was fabricated.

Hydrothermal fabrication of FeOOH/NiFe LDHs@CCH NAs-NF: The prepared CCH NAs-NF was used as substrate in this section. The precursor solution was

prepared by dissolving $Fe(NO_3)_2$ (0.1182 g), NH_4F (0.03552 g), and $CO(NH_2)_2$ (0.1152 g) in deionized water (70 mL) followed by 30 min stirring to ensure the homogeneity. The pH of the precursor solution should be carefully controlled around 10. The resultant solution was then transferred into a 80 mL Teflon-lined stainless steel autoclave. CCH NAs-NF was immersed into the precursor solution vertically. The autoclave was then sealed and transferred in an electric oven maintained at 120 °C for 5 h. After that, the autoclave cooled down naturally. The resultant sample was rinsed with deionized water and absolute ethanol to remove the residual reactants and dried in air. and accordingly the FeOOH/NiFe LDHs@CCH NAs-NF was fabricated.

Hydrothermal fabrication of FeOOH/NiFe LDHs-NF: NF was sonicated in HCl solution (30 wt.%) for 10 min to remove the nickel oxides on the surface, rinsed with deionized water and ethanol, then left dry in air. The precursor solution was prepared by dissolving $Fe(NO_3)_2$ (25 mM), $Ni(NO_3)_2$ (25 mM), NH_4F (0.2 M), and $CO(NH_2)_2$ (0.1 M) in deionized water (40 mL) followed by 30 min stirring to ensure the homogeneity. The resultant solution was then transferred into a 80 mL Teflon-lined stainless steel autoclave. NF was immersed into the as-prepared solution vertically. The autoclave was then sealed and transferred in an electric oven maintained at 120 °C for 5 h. After that, the autoclave cooled down naturally. The resultant sample was rinsed with deionized water and absolute ethanol to remove the residual reactants and dried in air, and accordingly the FeOOH/NiFe LDHs-NF was fabricated.

Materials Characterizations: The phase analysis of the sample was measured by X-ray diffraction (XRD, PANalytical X'Pert PRO) via Cu-Kα tube, operated at 40 kV,

and 40 mA. The scanning rate was 10^{o} min^{-1} from 20 ^{o} to 90 ^{o} in 2θ. Scanning electron microscopy (SEM) images and energy-dispersive X-ray analysis (EDX) were obtained using a JSM-7800F field emission scanning electron microscope (FE-SEM). The TEM images of the samples were further analyzed on a JEM-2000EX electron microscope, operated at an acceleration voltage of 120 kV. X-ray photoelectron spectra (XPS) were obtained on an Thermofisher ESCALAB 250Xi X-ray photoelectron spectrometer with Al Kα, hυ=1486.6eV，15kV，10.8mA. The binding energies achieved in the XPS spectral analysis were corrected for specimen charging by referencing C1s to 284.8 eV.

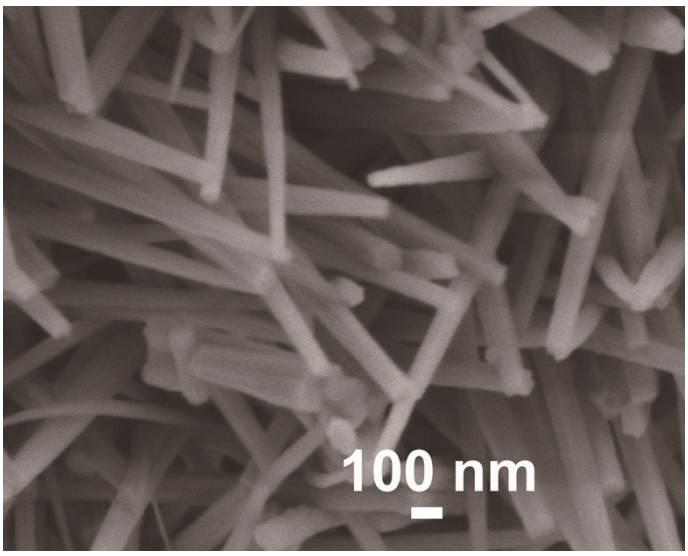

Figure S1. FE-SEM images of cobaltous carbonate hydroxide nanowires.

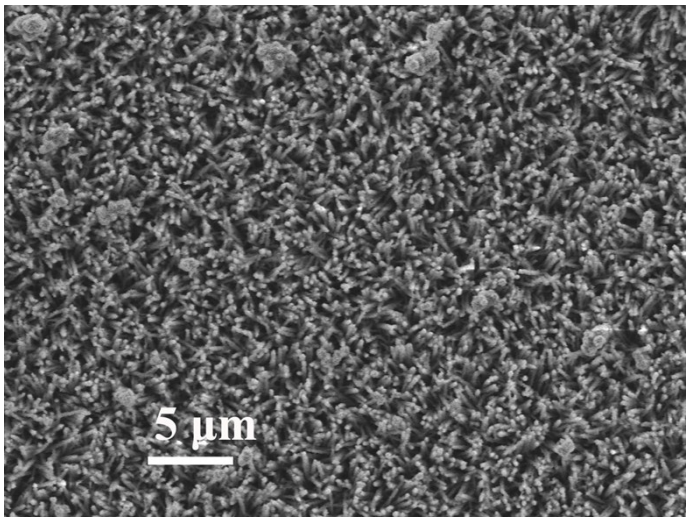

Figure S2. FE-SEM images of FeOOH/NiFe LDHs@CCH NAs-NF.

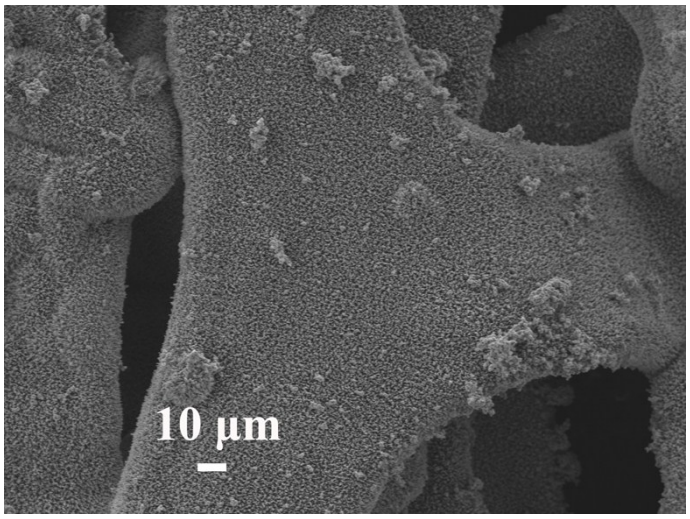

Figure S3. FE-SEM images of FeOOH/NiFe LDHs@CCH NAs-NF.

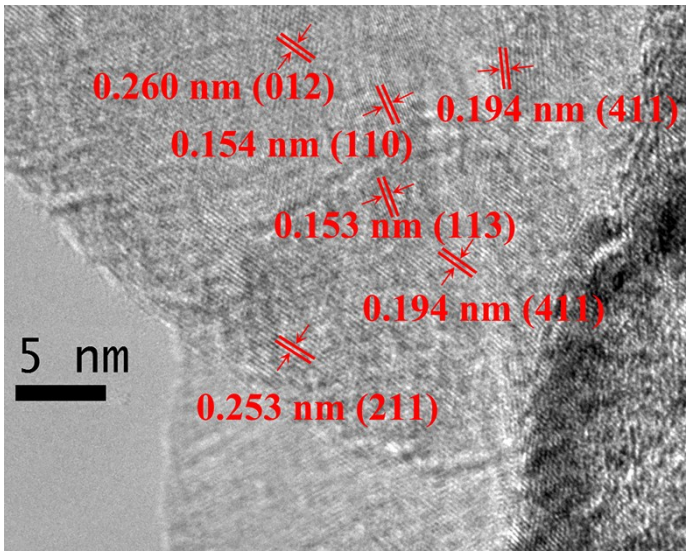

Figure S4. HR-TEM image of FeOOH/NiFe LDHs@CCH NAs-NF (scraped from the FeOOH/NiFe LDHs@CCH NAs-NF).

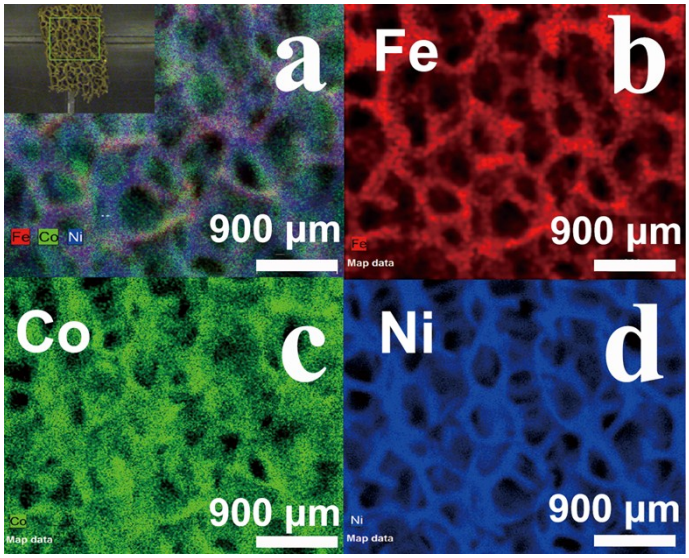

Figure S5. XRF images of the corresponding elemental mapping of Fe, Co, Ni, respectively,

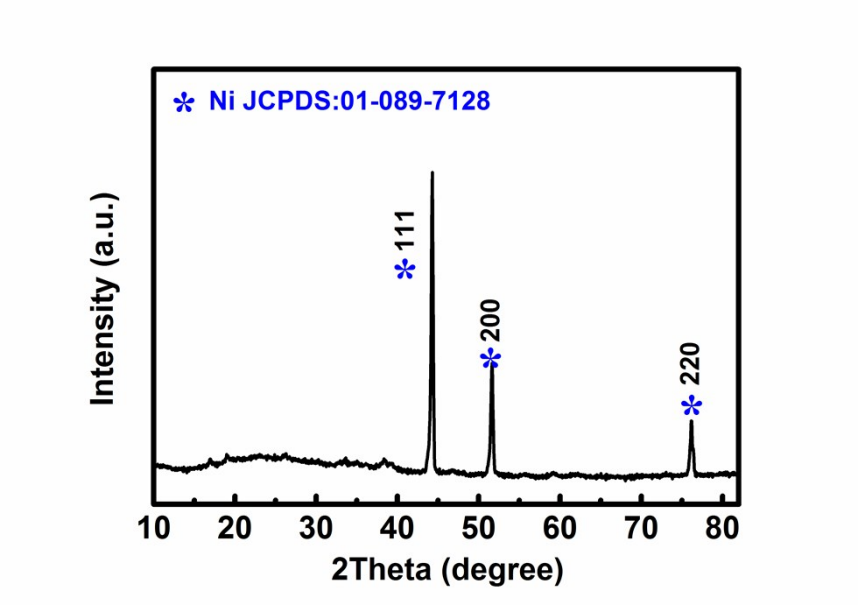

Figure S6. XRD patterns of FeOOH/NiFe LDHs@CCH NAs supported on NF.

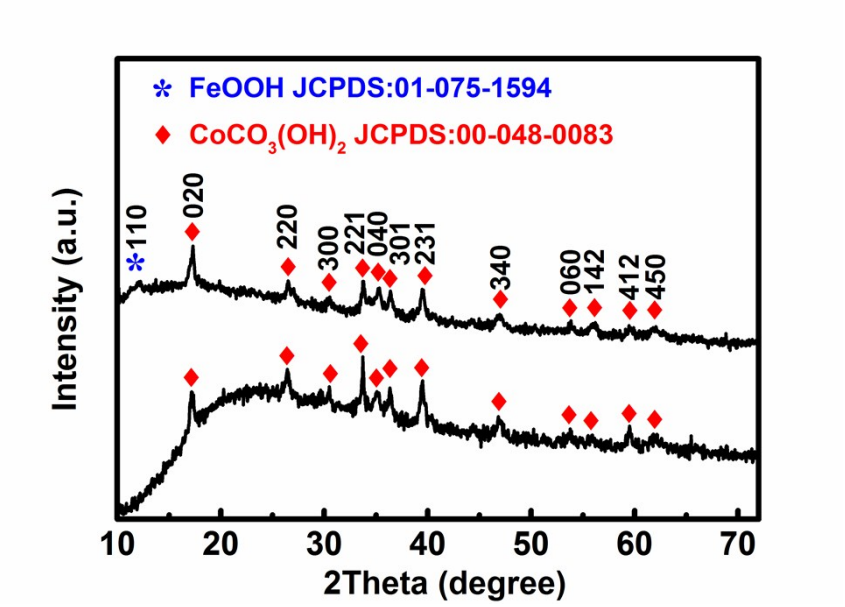

Figure S7. XRD patterns of FeOOH/NiFe LDHs@CCH NAs powders.

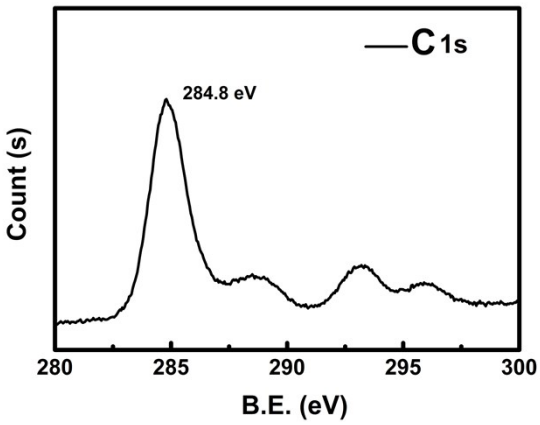

Figure S8. XPS spectrum of C 1s of FeOOH/NiFe LDHs@CCH NAs-NF.

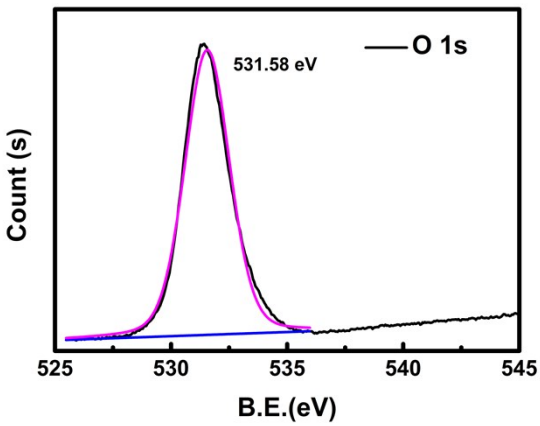

Figure S9. XPS spectrum of O 1s of FeOOH/NiFe LDHs@CCH NAs-NF.

S2 Electrochemical Measurements:

Reference electrode calibration: All of the electrochemical tests were carried out in a three-electrode system on an electrochemical workstation (Gamry Interface 5000E). The calibration was performed in the hydrogen saturated 1.0 M KOH with a Pt foil as the working electrode.

Mercuric oxide electrode (MMO) (1.0 M KOH) was used as the reference electrode in all measurements. The calibration was performed in the hydrogen saturated 1.0 M KOH, 25 ^{o}C with a Pt foil as the working electrode[1]. CVs were recorded at a scan rate of

1 mV s^{-1}. The potentials reported in our work were referenced to the RHE.

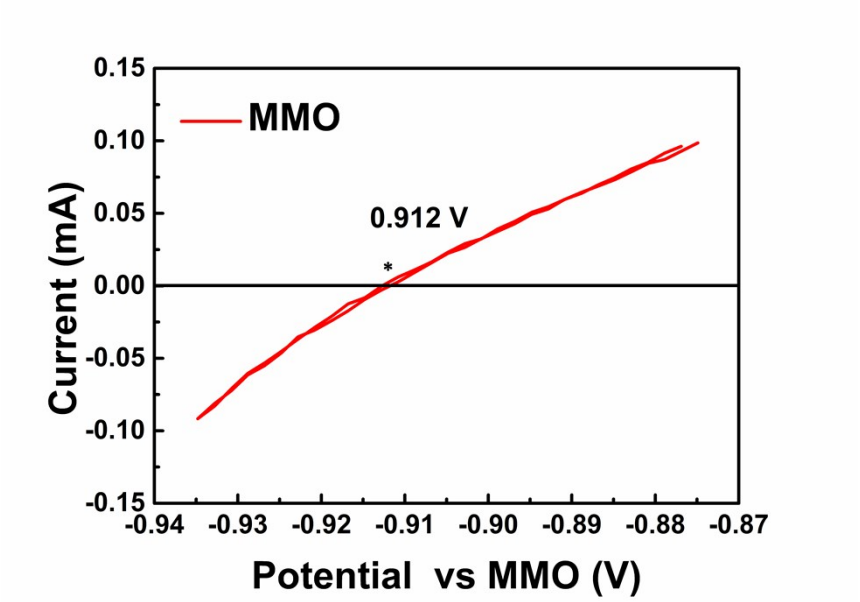

Figure S10. Calibration of MMO in H_2 saturated 1.0 M KOH.

E (V vs. RHE) = *E* (V vs. MMO) + 0.912 V.

Three-electrode measurements: To study the electrocatalytic activity and stability, the polarization curves was tested from overpotential from 0 V to 1 V vs MMO at 5 mV/s in 1 M KOH. The chronoamperometry measurements were carried out at 10-240 mA cm^{-2} in the solution of 1.0 M KOH (pH=14). Prior to all experiments, the electrolyte solution was purged with high purity O_2 gas for 30 min. For comparison study, all electrodes were also measured under the similar conditions. All

electrochemical measurements were carried out at 25 °C. Unless specifically mentioned, the voltammograms were recorded without *iR*-correction.

The electrocatalytic activity of FeOOH/NiFe-LDHs powders was evaluated on a rotating disk electrode (RDE), in a typical three-electrode configuration on a 4 mm glassy carbon disk electrode in O_2-saturated 1 M KOH electrolyte. A Pt slice (1×1 cm^2) and a MMO served as the counter and reference electrodes, respectively.

The fabrication of working electrode was as follows: 5 mg of sample was dispersed in 1 mL ethanol, followed by the addition of 20 μL 5% Nafion solution. The mixture was then ultra-sonicated for about 0.5 h to obtain a homogeneous ink. 5 μL the resulting ink was carefully dropped onto the RDE, leading to a catalyst loading of ~0.2 mg cm^{-2}. The as prepared catalyst film was dried at room temperature. *i-V* curve was recorded in 1 M KOH electrolytes with a scan rate of 10 mV s^{-2} at 25 ^oC.

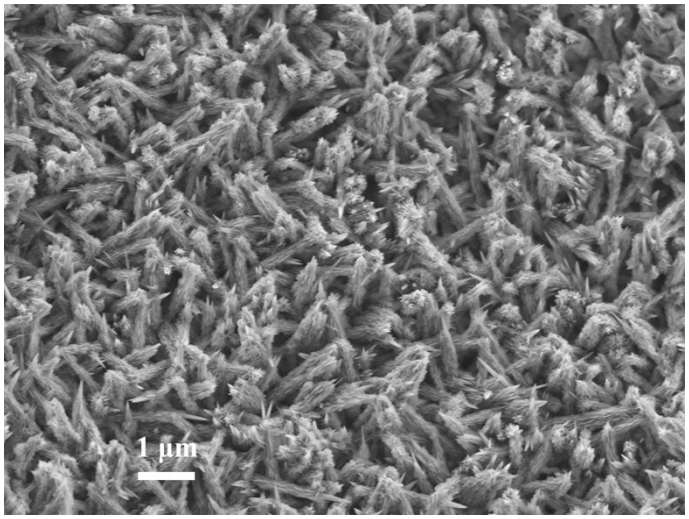

Figure S11. SEM images of FeOOH/NiFe LDHs@CCH NAs-NF after stability test in a standard three-electrode system at 25^oC.

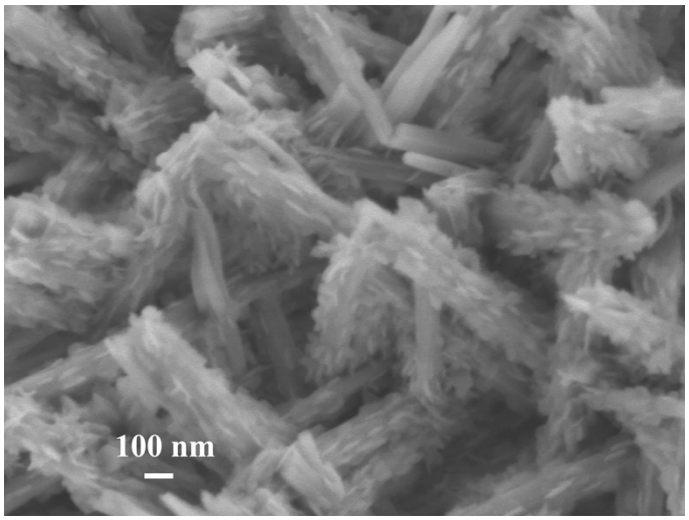

Figure S12. SEM images of FeOOH/NiFe LDHs@CCH NAs-NF after stability test in a standard three-electrode system at 25°C.

Double-layer capacitance measurements: The electrochemical active surface area (ECSA) of electrode is usually studied by the double layer capacitance [2-4]. Cyclic voltammograms in the double layer region (0.05-0.15 V vs open circuit potential) of FeOOH/NiFe LDHs@CCH NAs-NF, FeOOH/NiFe LDHs-NF, CCH NAs-NF, and Bare NF were recorded at different scan rates (0.025, 0.05, 0.08, 0.1, 0.15, 0.2, 0.4, 0.6, and 0.8 V s^{-1}). Cyclic voltammograms as shown in Figure S7-S10. The charging current, i_c, is then measured from CVs at multiple scan rates. The double-layer capacitance of electrode is calculated via equation (1).

$$i_c = v*C_{dl} \quad (1)$$

Thus, a plot of i_c as a function of v yields a straight line with a slope equal to C_{dl}.

The ECSA is calculated from the double-layer capacitance according to (2).

$$ECSA = C_{dl} / C_s \quad (2)$$

Where C_s is the specific capacitance of the sample or the capacitance of an atomically smooth planar surface of the material per unit area under identical electrolyte conditions. Amount of ECSA change depends linearly on the value of C_s for a specific material [4].

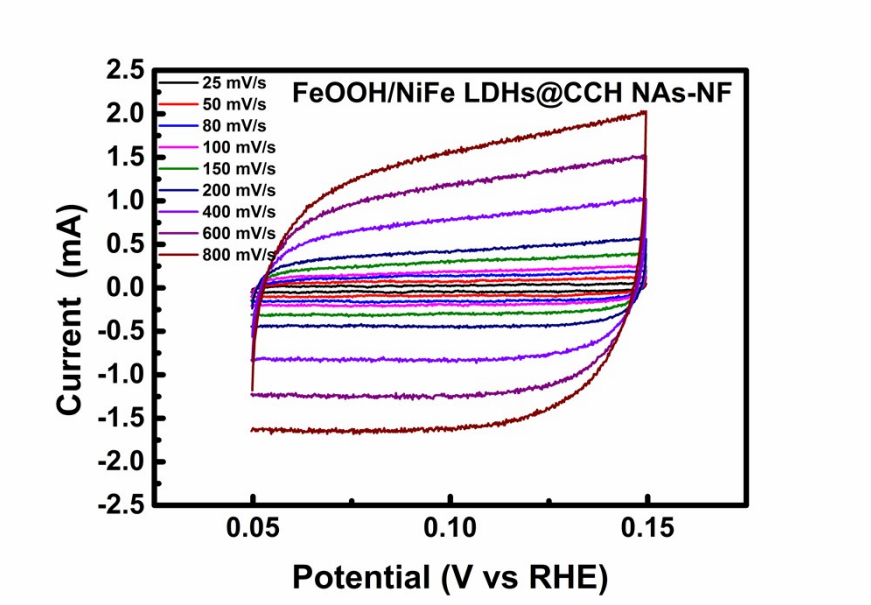

Figure S13. Cyclic voltammograms of FeOOH/NiFe LDHs@CCH NAs-NF were measured in a non-Faradaic region of the voltammogram at different scan rates in O_2 saturated 1.0 M KOH.

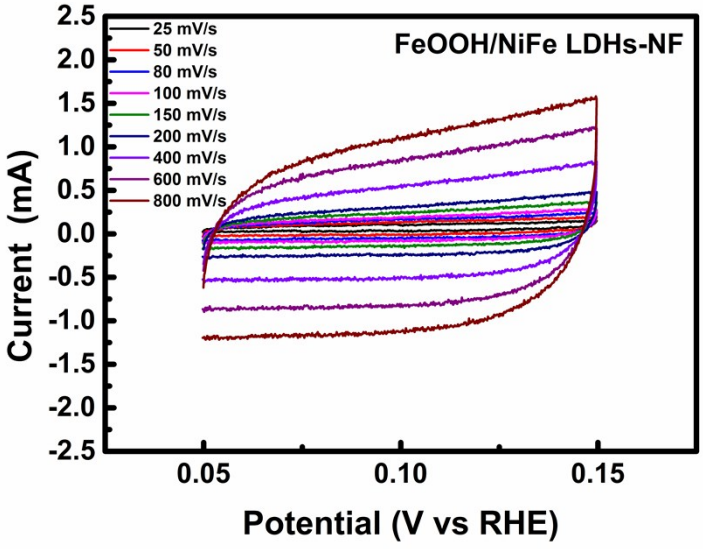

Figure S14. Cyclic voltammograms of FeOOH/NiFe LDHs-NF were measured in a non-Faradaic region of the voltammogram at different scan rates in O_2 saturated 1.0 M KOH.

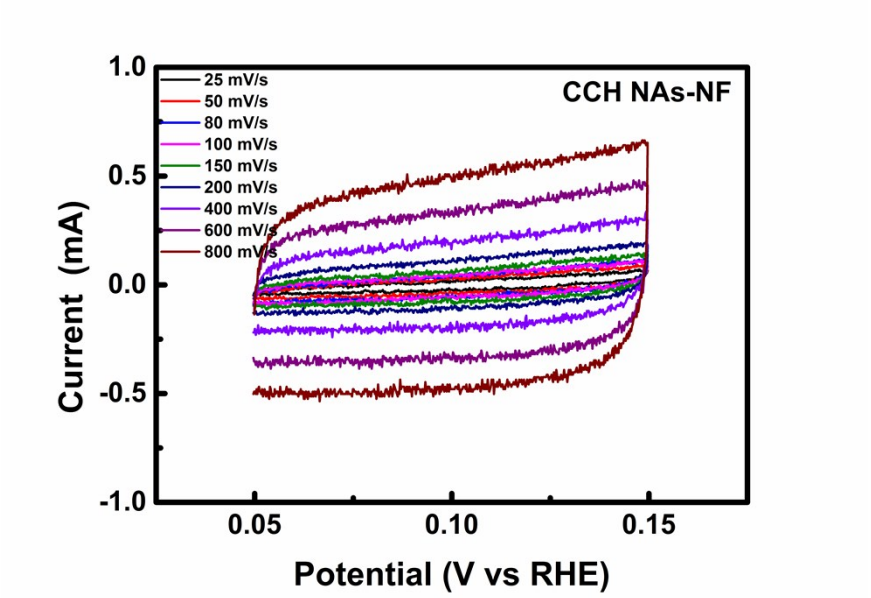

Figure S15. Cyclic voltammograms of CCH NAs-NF were measured in a non-Faradaic region of the voltammogram at different scan rates in O_2 saturated 1.0 M KOH.

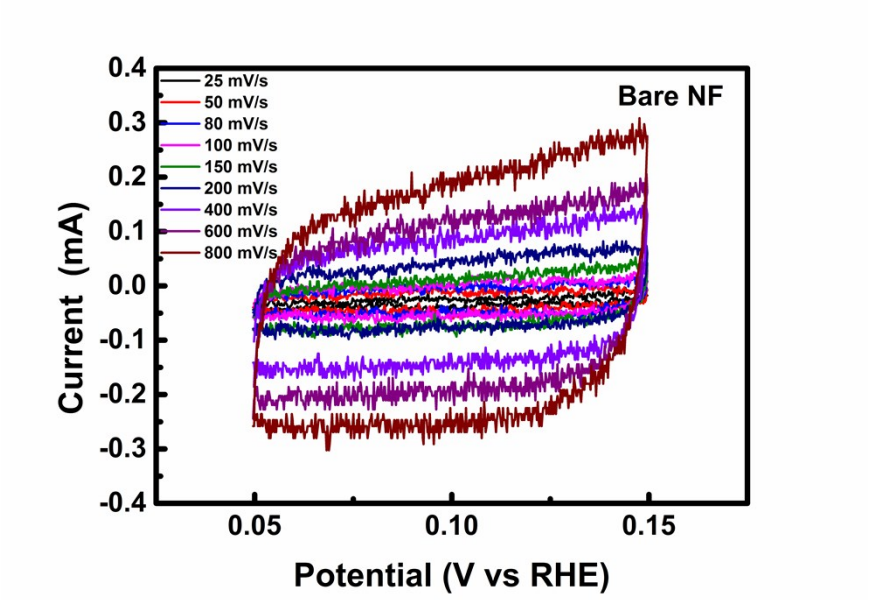

Figure S16. Cyclic voltammograms of Bare NF were measured in a non-Faradaic region of the voltammogram at different scan rates in O_2 saturated 1.0 M KOH.

Alkaline polymer electrolyte water electrolysis tests*:* To evaluate the OER performance of the prepared catalyst in real electrolysis, alkaline polymer electrolyte water electrolyzer (APEWE) (2×1.5 cm^2) were assembled. The prepared FeOOH/NiFe LDHs@CCH NAs-NF was used as the anode. A wet-proof carbon paper loaded with 0.4 mg cm^{-2} Pt/C (70 wt.% Pt/C, Johnson Matthey) was used as the cathode. An alkaline polymer electrolyte (APE) membrane (home-made) was chosen as the solid polymer electrolyte. The catalyst coated membrane and cathode were then hot-pressed at 60^{o}C and 0.2 MPa for 1 min. The steady-state *i-V* tests were conducted at 70 ^{o}C in potentiostatic mode. The stability test was performed at 500 mA cm^{-2} and 70 ^{o}C, 1.0 M KOH solution was supplied to the anode compartment at 5 mL min^{-1}.

Table S1. Summary results for representative non-precious-metal OER electrocatalysts reported in the literatures.

Catalyst	Electrolyte	Overpotential at 10 mA cm^{-2} (η_{10},mV)	Overpotential at 100 mA cm^{-2} (η_{100},mV)	Reference
FeOOH/NiFe LDHs@CCH NAs-NF	1.0 M KOH	220	290	This work
Fe LDHs-NF	1.0 M KOH	258	364	This work
Co_3O_4 @MWCNT	1.0 M KOH	309		5
$NiCo_2O_4$ Hollow Microcuboids	1.0 M NaOH	420		6
Ni_3Se_2 nanoforest/NF	1.0 M KOH	242[(a)] (η_{20})	353[(a)]	7
Cobalt Nitride Nanowires-NF	1.0 M KOH	290[(a)]		8
Ni^{2+}/MnO_2	1.0 M KOH	400		9
FeO_x/CFC after OER for 15 h	1.0 M KOH	431[(a)]	514[(a)]	10
CoMnP nanoparticles	1.0 M KOH	330[(a)]		11
NiFe/NF	1.0 M KOH	215[(a)]	270	12

			(30 wt% KOH)	
Porous NiFe/$NiCo_2O_4$ /Ni Foam	1.0 M KOH	240[b]	380[c]	13
FeOOH/Co/FeOOH HNTAs-NF	1 M NaOH	250(η_{21})	300(η_{91})	14
FeOOH/Co/FeOOH HNTAs-NF	1 M NaOH	350(η_{199})	300(η_{91})	14

a) Data with iR-compensation; b) Onset overpotential; c) This value is not mentioned in the literature but derived from the LSV results.

Table S2. Summary results for representative non-precious-metal APEWE reported in the literatures.

Anode Cathode	Tempareture °C	Electrolyte	Potential at 100,500 mA cm^{-2} (V_{100}, V_{500} V)	Durability test(h)	Reference
FeOOH/NiFe LDHs@CCH NAs-NF 0.5 mg_{Pt} cm^{-2} Pt/C	70	1.0 M KOH	1.51 1.768	100 I=500 mA cm^{-2}	This work
1.85μg_{Pt} cm^{-2} Pt-Ni/CP-2 Ni/CP	70	1.0 M KOH	1.66[a] 1.87[a]	Not mentioned	15
Ni/Zn/S-GO Ni/Zn/S-GO	80	5.36 M KOH	Not mentioned 1.89[a]	20 I= ~500 mA cm^{-2}	16
85μg_{Ni} cm^{-2} Ni/CP 85μg_{Ni} cm^{-2} Ni/CP	70	1.0 M KaOH	1.70[a]	Not mentioned	17
4.8 mg cm^{-2} Acta 3030 7.4 mg cm^{-2} Acta 43030	43	1 wt.% K_2CO_3	1.70[a] 1.92[a]	800 I= 470 A cm^{-2}	18
2.9 mg cm^{-2} IrO2 3.2 mg cm^{-2} Pt	50	deionized water	1.56[a] 1.86[a]	500 I=200 mA cm^{-2}	19
NiFe-Anode NiMo-Cathode	80	deionized water	1.69[a] 1.88[a]	8 I=400 mA cm^{-2}	20

a) This value is not mentioned in the literature but derived from the LSV results.

References

1. Y. L. Yongye Liang, HailiangWang, Jigang Zhou, JianWang, Tom Regier and Hongjie Dai*, *Nat. Mater.*, 2011, **10**, 780-786.
2. C. C. McCrory, S. Jung, I. M. Ferrer, S. M. Chatman, J. C. Peters and T. F. Jaramillo, *J. Am. Chem. Soc.*, 2015, **137**, 4347-4357.
3. R. Chen, H.-Y. Wang, J. Miao, H. Yang and B. Liu, *Nano Energy*, 2015, **11**, 333-340.
4. C. C. McCrory, S. Jung, J. C. Peters and T. F. Jaramillo, *J. Am. Chem. Soc.*, 2013, **135**, 16977-16987.
5. Y.-X. Zhang, X. Guo, X. Zhai, Y.-M. Yan and K.-N. Sun, *J. Mater. Chem. A*, 2015, **3**, 1761-1768.
6. X. Gao, H. Zhang, Q. Li, X. Yu, Z. Hong, X. Zhang, C. Liang and Z. Lin, *Angew. Chem., Int. Ed.*, 2016, **55**, 6290-6294.
7. R. Xu, R. Wu, Y. Shi, J. Zhang and B. Zhang, *Nano Energy*, 2016, **24**, 103-110.
8. Y. Zhang, B. Ouyang, J. Xu, G. Jia, S. Chen, R. S. Rawat and H. J. Fan, *Angew. Chem. Int. Ed.*, 2016, DOI: 10.1002/anie.201604372.

9. A. C. Thenuwara, E. B. Cerkez, S. L. Shumlas, N. H. Attanayake, I. G. McKendry, L. Frazer, E. Borguet, Q. Kang, R. C. Remsing, M. L. Klein, M. J. Zdilla and D. R. Strongin, *Angew. Chem. Int. Ed. Engl.*, 2016, **55**, 1-6.
10. F. Yan, C. Zhu, S. Wang, Y. Zhao, X. Zhang, C. Li and Y. Chen, *J. Mater. Chem. A*, 2016, **4**, 6048-6055.
11. H. B. Da Li, Cláudio N. Verani, and Stephanie L. Brock*, *J. Am. Chem. Soc.*, 2016, **138**, pp 4006–4009.
12. X. Lu and C. Zhao, *Nat Commun*, 2015, **6**, 6616.
13. C. Xiao, Y. Li, X. Lu and C. Zhao, *Adv. Funct. Mater.*, 2016, **26**, 3515-3523.
14. J. X. Feng, H. Xu, Y. T. Dong, S. H. Ye, Y. X. Tong and G. R. Li, *Angew. Chem. Int. Ed.*, 2016, **55**, 3694-3698.
15. S. H. Ahn, S. J. Yoo, H.-J. Kim, D. Henkensmeier, S. W. Nam, S.-K. Kim and J. H. Jang, *Applied Catalysis B: Environmental*, 2016, **180**, 674-679.
16. S. Seetharaman, R. Balaji, K. Ramya, K. S. Dhathathreyan and M. Velan, *Int. J. Hydrogen Energy*, 2013, **38**, 14934-14942.
17. S. H. Ahn, B.-S. Lee, I. Choi, S. J. Yoo, H.-J. Kim, E. Cho, D. Henkensmeier, S. W. Nam, S.-K. Kim and J. H. Jang, *Applied Catalysis B: Environmental*, 2014, **154-155**, 197-205.
18. F. C. Claudiu C. Pavel, Chiara Emiliani, Serena Santiccioli, Adriana Scaffidi,Stefano Catanorchi, and Massimiliano Comotti*, *Angew. Chem.*, 2014, **53**, 1378 –1381.
19. Y. Leng, G. Chen, A. J. Mendoza, T. B. Tighe, M. A. Hickner and C. Y. Wang, *J. Am. Chem. Soc.*, 2012, **134**, 9054-9057.
20. L. Xiao, S. Zhang, J. Pan, C. Yang, M. He, L. Zhuang and J. Lu, *Energy Environ. Sci.*, 2012, **5**, 7869.